Comparison of Computer Predictions and Field Data for Dynamic Analysis of Falling Weight Deflectometer Data

ALLEN H. MAGNUSON, ROBERT L. LYTTON, AND ROBERT C. BRIGGS

The extraction of engineering properties of pavement layers by dynamic analysis of falling weight deflectometer (FWD) data is demonstrated. FWD data from two in-service highway sections were analyzed. The FWD data consist of time records of surface loading and surface deflections at a range of distances. A Texas Transportation Institute pavement dynamics computer program, SCALPOT, was used to generate predicted responses. Physical properties of the pavement were generated by a trial-and-error backcalculation and a Systems Identification computer program. The pavement surface vertical deflections were characterized by using frequency response functions in the form of magnitude and phase angle plots as a function of frequency. The magnitude plots represent vertical pavement surface deformations resulting from a steady-state sinusoidal surface loading. The phase angle data represent the lag angle between the loading and the surface deflections. The asphaltic concrete surface layer was represented as a three-parameter viscoelastic medium. The base course, subgrade layers, and bedrock layers, if any, were treated as damped elastic solids. These physical properties were backcalculated by matching approximately the frequency-analyzed field data with computed values by varying the SCALPOT input data set. Good agreement between experimental and computer-predicted responses was obtained using the backcalculated pavement layer properties. One site with near-surface bedrock was analyzed and good agreement was obtained.

Dynamic analysis is governed by various forms of Newton's second law. In continuum mechanics Newton's law is usually expressed as the Navier vector field equation. For an axisymmetric, horizontally layered, viscoelastic medium (a highway pavement section), the vector field equation can be separated into two scalar reduced wave equations, each having its own scalar potential. The equations can be solved readily by using separation of variables and a suitable orthonormal eigenfunction expansion. The expanded solution can be evaluated numerically with specially formulated computer algorithms, which may be implemented in one or more computer programs. This process has been completed for the pavement dynamics problem, and some initial results are presented.

Dynamic analysis requires understanding of creep compliance functions, complex moduli, wave phenomena, dynamic vector field equations, compressional waves, shear waves, layered media, and many other physical phenomena, as well as various applied mathematics disciplines and numerical methods. By contrast, static analysis is usually formulated using the biharmonic operator, which is a special case (zero frequency) of the two reduced wave operators in the corresponding dynamic formulation.

A. H. Magnuson and R. L. Lytton, Texas Transportation Institute, Texas A&M University System, College Station, Tex. 77843. R. C. Briggs, Texas State Department of Highways and Public Transportation, Austin, Tex. 78701.

NEED FOR PAVEMENT DYNAMIC ANALYSIS

One may well ask, Why use dynamic analysis when static analysis methods are readily available? What, if anything, is wrong with existing static analysis procedures? These questions can be answered as follows:

- Dynamic analysis is more accurate and physically realistic, because it takes into account transient (time-dependent) wave phenomena in the pavement layers.
- More information on pavement layer properties can be extracted, because all the information in the falling weight deflectometer (FWD) time-pulse data is used in the backcalculation procedure (as opposed to only peak values of the pulses, as is currently done in elasto-static analysis).
- With dynamic analysis, the viscoelastic properties of the asphaltic concrete (AC) surface layer can be characterized by creep compliance functions in the time domain and complex moduli in the frequency domain. Static analysis is limited to elastic modeling because viscoelastic phenomena are inherently dynamic.
- More physical insight into the pavement section (e.g., the presence of bedrock, modal responses, and reflection and refraction between layers) can be obtained from dynamic analysis.
- Dynamic analysis is more sensitive to pavement layer properties because of the additional data available. This means that, in principle, more accurate backcalculation results can be obtained.

Dynamic analysis potentially offers the following benefits: cost savings, fast response time, and additional engineering information. Among the inherent advantages of FWD dynamic analysis are nondestructive testing of the pavement surface and inexpensive, fast automated data acquisition and analysis.

BACKGROUND

In September 1987 the Materials, Pavements and Construction Division of Texas Transportation Institute (TTI) started

work on a 4-year research project, "Dynamic Analysis of Falling-Weight Deflectometer Data." The project is administered by the Texas State Department of Highways and Public Transportation as part of FHWA's Cooperative Research Program. The project's purpose is to develop a computer model of pavement dynamic response and to apply it in the prediction and evaluation of pavement performance.

The division is using mechanistic approaches to characterize pavement failure and aging associated with cracking and rutting. The dynamic analysis of FWD data can, in principle, be used to backcalculate pavement layer properties related to remaining pavement life.

FWD (or drop weight force impulse) devices are in widespread use for in-service pavement evaluation and backcalculation of moduli. However, pavement response data are currently analyzed with static models.

In static analysis the dynamic deflection basin caused by the FWD is assumed to be static, whereby the instantaneous pavement deflection at a given point is assumed to be proportional to the instantaneous force on the pavement surface. In static analysis, therefore, only the peak values of the force and deflection pulses are used.

The FWD time-pulse data contain much more information on the pavement layers; however, this information cannot be extracted without a working pavement dynamic analysis program. Static analysis methods are used because no one has yet developed a practical working dynamic analysis program for pavements.

RELATED WORK

Pavement impulse testing is described by Lytton et al. (*1*) and Uzan et al. (*2*). Dynamic response of geophysical and geotechnical systems started with the work of Lamb (*3*), who solved the problem of the dynamic response of a uniform half-space to describe the main features of earthquake tremors. Ewing et al. (*4*) is a standard reference in seismology for dynamic analysis of multilayered elastic media. The analysis used in TTI's SCALPOT computer program is a direct extension of this work.

Magnuson (*5,6*) developed a matrix recurrence relation to solve the multilayered viscoelastic problem for another application. The recurrence relation reduced the matrix relations to a series of 4 × 4 matrix manipulations that could easily be programmed on a computer. He also introduced viscoelastic complex moduli into the multilayer problem by using the correspondence principle. Each layer's response was characterized by two scalar potentials, one for the compressional wave and the other for the vertical shear wave. The solution is expressed as a Fourier-Bessel integral expansion. This expression is an improper integral having one or more pole singularities near the path of integration and an infinite upper limit. The integral is particularly difficult to evaluate accurately because of the slow convergence as the upper limit approaches infinity. Magnuson (*7*) describes an integration algorithm developed for the pavement dynamics problem. The algorithm is an extension of Zhongjin's analysis (*8*). The multilayered medium's matrix algebra (*6*) and the integration algorithm (*7*) have been incorporated into the SCALPOT computer program, which was developed for the dynamic analysis of pavement responses.

SCALPOT AND FWD-FFT

The SCALPOT (scalar potential) program developed at TTI computes the dynamic response of a horizontally layered viscoelastic half-space to a time-dependent surface pressure distribution. Vertical surface deflections resulting from the oscillatory surface pressure distribution can be obtained for a range of frequencies and distances from the surface pressure distribution.

SCALPOT has been modified to incorporate a surface layer. Additional modifications were made to treat pavement sections with stiff layers and near-surface bedrock. The input data set for SCALPOT consists of the geometrical configuration of the FWD apparatus and the physical properties of each pavement layer. The properties of each layer include thickness, weight density, viscoelastic parameters, Young's modulus, damping ratio, and Poisson's ratio. SCALPOT is currently programmed to treat each layer as a damped elastic solid or as a three-parameter viscoelastic medium.

Another computer program developed at TTI, FWD-FFT, was used for analyzing the FWD data. The methods used to analyze the FWD data are described elsewhere (*9*). The program scans the time series data, makes the pulse "tail correction," computes averages, and performs a Fast Fourier Transform (FFT) of the corrected and averaged pulse data. FWD frequency response functions are then computed by performing a complex division of the FFT of the surface deflections by the FFT of the surface loading. The frequency response functions are computed for the seven displacements at each site, and the results are written to data files and plotted.

FREQUENCY DOMAIN ANALYSIS

FWD time pulses are transformed to the frequency domain by using the superposition principle. The transient pulses are expressed as a sum of time-harmonic functions interfering with each other in such a way as to closely replicate the original pulse shape. This process is performed efficiently using FFTs, which are based on an algorithm formulated by Cooley and Tukey in the 1960s.

This study was conducted using frequency domain analysis, whereby the pavement surface vertical deflections were characterized with steady-state frequency response functions. At a given frequency, the vertical surface deflections are represented as the response to a sinusoidal vertical surface loading. The data are presented in the form of magnitude and phase angle plots as a function of frequency. The phase angle represents the lag angle (at a given frequency) between the loading and the surface deflections.

PAVE-SID

PAVE-SID, a computer program based on the System IDentification (SID) methodology, was developed to extract pavement properties by using FWD data and dynamic analysis techniques. PAVE-SID is described by Torpunuri (*10*). The inputs to the program are the FWD experimental frequency response functions and computed responses generated by the

SCALPOT program. The SID method is described in detail elsewhere (*11,12*). PAVE-SID uses SCALPOT to generate a data base for constructing a sensitivity matrix. Increments in pavement layer properties are computed from the field data and the sensitivity matrix. The updated parameters are input into SCALPOT, and the response is computed and compared against the field data. The process is repeated until convergence is obtained.

PAVEMENT VISCOELASTIC PROPERTIES

An early study of viscoelastic properties of AC materials was conducted by Papazian (*13*). Papazian performed laboratory creep tests on AC core samples and used a linear Voigt-chain-Maxwell viscoelastic representation (*14*) to model the strain data in both the time and frequency domains. Lai and Anderson (*15*) used a nonlinear Voigt-chain-Maxwell viscoelastic representation to model the creep and recovery of AC material.

Paris's law governing crack propagation in a viscoelastic medium provides a direct link between pavement cracking and physical properties of the AC material. Schapery (*16*) put Paris's law on a sound mechanistic footing and developed a nonlinear fracture theory for viscoelastic composite materials applicable to AC pavements.

Pavement rutting resulting from permanent deformation of the AC layer is characterized by Kenis's viscoelastic system (VESYS) mu-alpha formulation (*17*). The VESYS formulation can be applied to the viscoelastic characterization of the pavement to estimate remaining life before failure from rutting.

ANALYSIS OF FWD DATA

Figure 1 is a time plot of the FWD forces and surface deflections for the District 1, Site 3 (D01S3) pavement section near Paris, Texas. Figure 2 is a similar plot for the District 8, Site 4 (D08S4) section (Interstate 20) near Abilene, Texas. The FWD data in Figures 1 and 2 are in the form of digitized time series with a sampling rate of 0.2 msec over a 60-msec duration. Figures 1 and 2 are working plots used in data reduction and preprocessing. They are screen dumps of a VGA 640- × 480-pixel color video display from an IBM AT-compatible computer with an Intel 30386 microprocessor. The forces and deflections are scaled from the pixel plots by dividing by the "fconst" and "dconst" values shown for each figure. The headers for each figure site give the load, highway section data, date of test, thickness of AC surface course, and surface temperature. The inverted curves at the tops of the figures show the drop weight force on the pavement surface as a function of time. The seven surface deflections are shown for sensors spaced 0, 1, 2, 3, 4, 5, and 6 ft from the center of the drop weight. The deflections decrease with distance, so the largest deflection is for the sensor at $r = 0$. The deflections in Figure 2 for D08S4 show an overshoot or zero-crossing at the tail of the pulse. The zero-crossings of the deflections indicate that near-surface bedrock is present.

CREEP COMPLIANCE DATA FROM AC SAMPLES

Core samples for the sections were taken in an earlier study. Information on the sections is given in Table 1, which indicates that they are both relatively stiff pavements having a thick AC surface course. Figure 3 shows recently obtained creep data for three AC core samples for the D01S3 and D08S4 sections. The data in Figure 3 show longitudinal strain response of the AC surface course samples subjected to a suddenly applied constant stress (step function) uniaxial compression. The data were taken using a materials testing system machine at TTI. The strain data in Figure 3 are presented in the form of log-log plots of millistrain as a function of time.

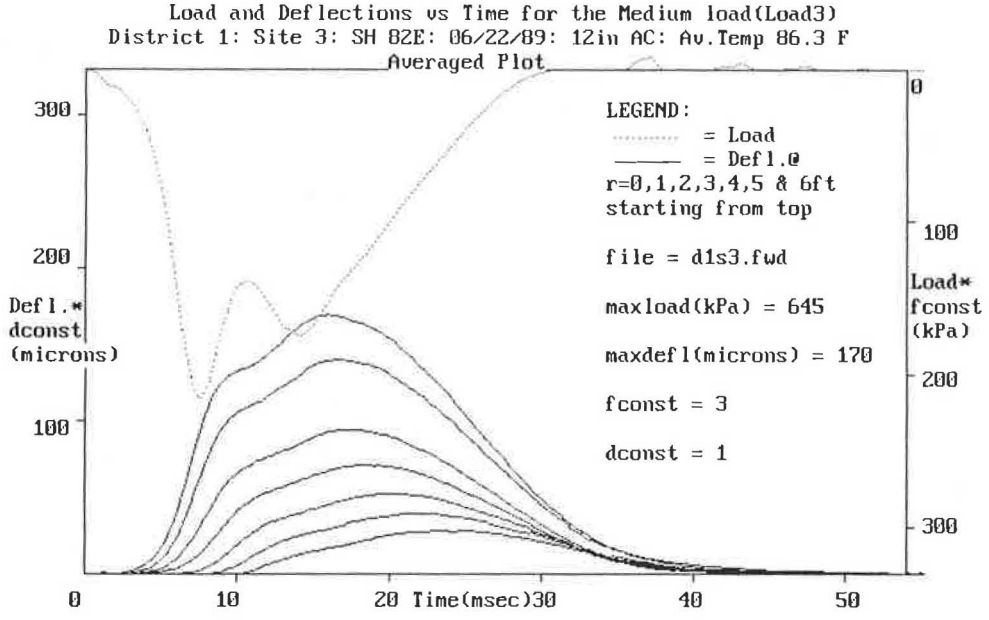

FIGURE 1 FWD time-pulse data, D01S3—drop weight force and seven displacement sensors versus time.

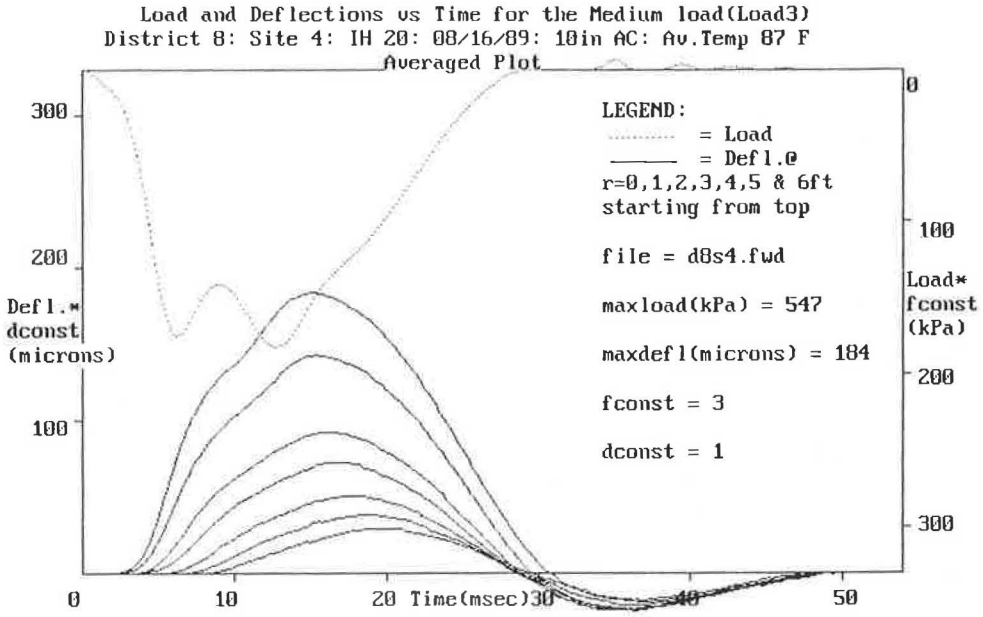

FIGURE 2 FWD time-pulse data, D08S4—drop weight force and seven displacement sensors versus time.

TABLE 1 PAVEMENT SECTION CHARACTERISTICS (FROM CORE SAMPLING LOG)

Section	Surface Course	Base Course	Subgrade
D01-S3	12 in thk AC	22 in (Sandy)	Clay
D08-S4	10 in thk AC	11 in LS CR	Clay:Rock @ 9.75 ft

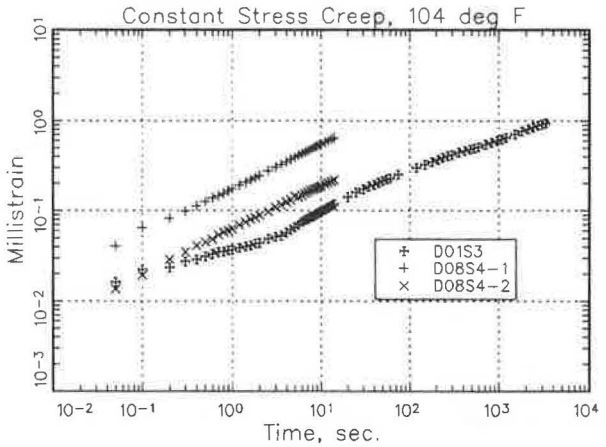

FIGURE 3 Log-log plots of millistrain from laboratory compressional creep tests—one sample from D01S3 and two samples from D08S4.

PAVEMENT FREQUENCY RESPONSE FUNCTIONS

Figures 4 and 5 represent the frequency response functions for pavement vertical surface deflections resulting from a vertical surface pressure distribution caused by the FWD apparatus. For convenience, the magnitude responses are given in units of mils per 10 kips in Figures 4a, 4c, 5a, and 5c. Figure 4 shows D01S3 frequency response functions computed from FWD data using the FWD-FFT computer program. Data are shown for displacements at r = 0, 1, 2, 3, 4, 5, and 6 ft. Magnitude responses for the inner sensors, phase angles for the inner sensors, magnitudes for the outer sensors, and phase angles for the outer sensors are shown in Figures 4a, 4b, 4c, and 4d, respectively. The magnitudes in Figures 4a and 4c decrease with r, so the r = 0 curve is on top, the r = 1 ft curve is immediately below it, and so on. The phase angle curves in Figures 4b and 4d start with the smallest r on top and work down as r increases.

These FWD frequency response curves behave the same for all the sections examined so far; the general arrangement of the response curves in Figure 4 is the same for other sections. The magnitude curves decrease with frequency because of the effect of the mass through Newton's law. Similarly, the phase angles increase with frequency.

The D01S3 phase angle curves for r = 5 and 6 ft show a jump at the higher frequencies. The jump coincides with a dip or partial null in the corresponding magnitude curves. This behavior indicates wave interference, or possibly modal response caused by repeated back reflection off lower layers.

Figure 5 shows D08S4 frequency response functions computed from FWD data using the FWD-FFT computer program. Data, which are shown for the same displacements as for Figure 4, are arranged in the same way as the data in

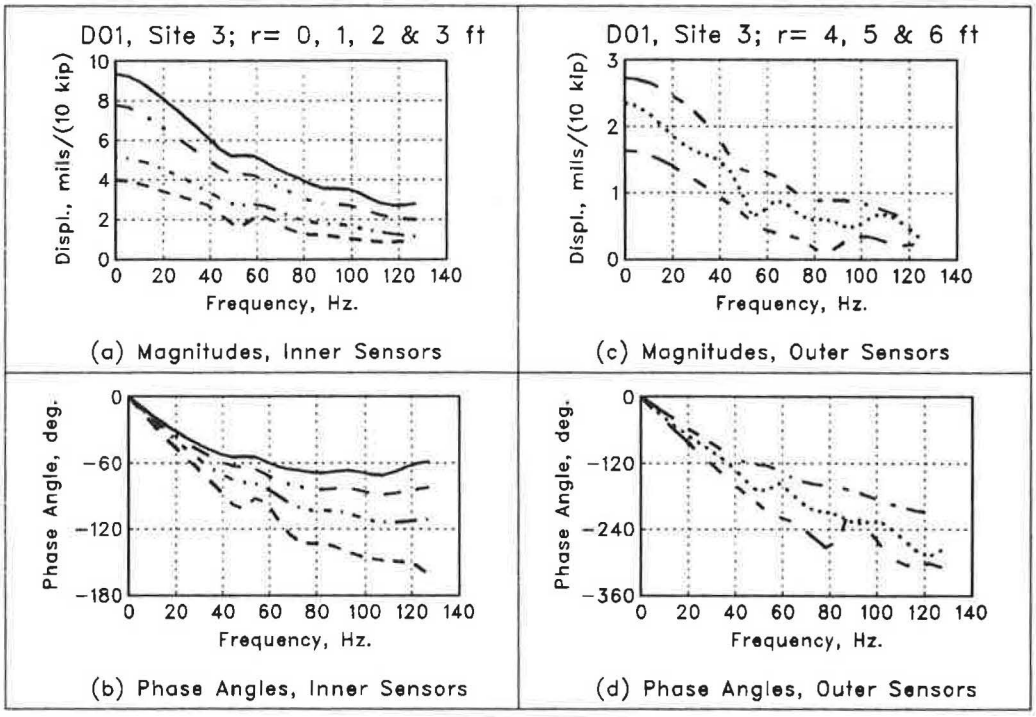

FIGURE 4 D01S3 frequency response functions (computed from FWD data).

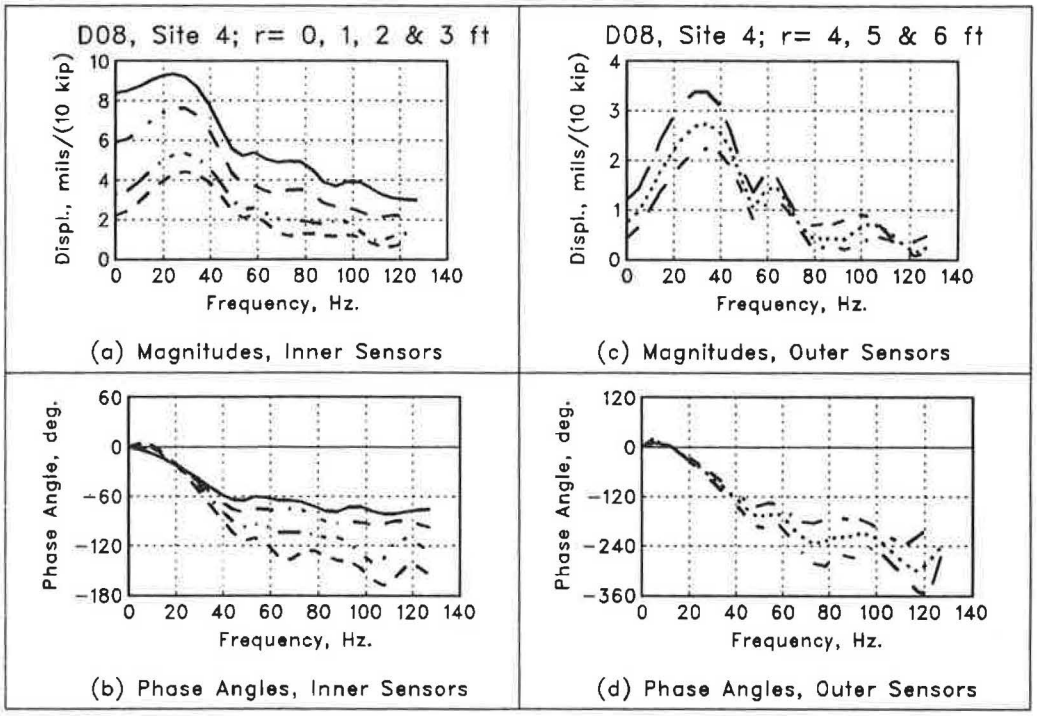

FIGURE 5 D08S4 frequency response functions (computed from FWD data).

Figure 4. The magnitude and phase angle curves differ considerably from the D01S3 responses because of the near-surface bedrock. The magnitude responses have a pronounced peak at about 30 Hz. The peaking increases for increasing distance r. There are two or three partial nulls in magnitude and corresponding jumps in phase angle. In addition the phase angles of the inner sensors show a crossover at about 25 Hz followed by a lead angle for lower frequencies. There is apparently a connection between the unusual behavior of the frequency response curves in the presence of bedrock and the time-pulse overshoot or zero-crossing seen in Figure 2.

VISCOELASTIC REPRESENTATION OF AC MATERIAL

The simplest way to interpret the data in Figure 3 is to use a two-parameter power-law representation, as follows:

$$D(t) = At^n \tag{1}$$

where n is the log-log slope and A is the intercept at $t = 1$ sec. A three-parameter representation, a generalized time-domain power-law representation, is also in extensive use. The generalized power-law or three-parameter representation separates the viscoelastic part from the (assumed) elastic response, and may be written as follows:

$$D(t) = D_0 + D_1t^n \tag{2}$$

where D_0 is the elastic compliance and D_1 is the viscoelastic term evaluated at $t = 1$ sec.

Because of the reciprocal relationship between compliances and moduli, the first and second compliances in Equation 2 can be written as follows:

$$D_0 = E_0^{-1} \tag{3a}$$

and

$$D_1 = E_1^{-1} \tag{3b}$$

where E_0 is the elastic modulus and E_1 is the viscoelastic modulus at $t = 1$ sec.

Expressing Equation 2 in terms of the moduli in Equation 3 gives

$$D(t) = 1/E_0 + t^n/E_1 \tag{4}$$

This representation, when evaluated at $t = 1$ sec, is equivalent to two springs in series.

FREQUENCY DOMAIN REPRESENTATION OF AC CREEP COMPLIANCE

The time-domain creep compliance functions (Equations 1 and 2) must be transformed into the frequency domain for use in pavement dynamic analysis programs. The frequency-domain representation is called the complex compliance because it can be expressed as a complex number having a real part and an imaginary part. Performing a Fourier integral transform on Equations 1 and 2 gives the following for the two- and three-parameter complex compliances, respectively:

$$D(\omega) = A\Gamma(1 + n)\omega^{-n}[\cos(n\pi/2) - i\sin(n\pi/2)] \tag{5a}$$

$$D(\omega) = D_0 + D_1\Gamma(1 + n)\omega^{-n}[\cos(n\pi/2) - i\sin(n\pi/2)] \tag{5b}$$

where $i = \sqrt{-1}$, ω is the radian frequency, and Γ represents the gamma function.

Equation 5b, for the three-parameter representation, has been coded into the SCALPOT program.

LABORATORY CREEP COMPLIANCE DATA

The D01S3 and D08S4 creep data in Figure 3 were used to obtain the viscoelastic parameters for the three-parameter model shown in Equation 2. For that representation, the constant D_0 for the elastic component is an assumed value. The viscoelastic component was obtained by subtracting out the assumed elastic term from the total creep data in Figure 3 and replotting the remaining strain on a log-log scale. The viscoelastic parameters n and D_1 are obtained from the slope and intercept, respectively, of the log-log plots.

DESCRIPTION OF COMPARISON STUDY

The comparison study presented here was conducted on Sections D01S3 and D08S4 because core samples from these sections were left over from a previous investigation. The samples were tested in uniaxial constant stress in compression. This allowed the investigators to compare backcalculated viscoelastic parameters obtained from FWD data with laboratory test results.

The frequency response functions shown in Figures 1 and 2 were compared with corresponding computed values generated by the SCALPOT program. The backcalculation study was performed by estimating the SCALPOT data set using creep data for AC materials and modulus data generated from static backcalculation efforts. The estimated data set was used in the SCALPOT program to obtain a first approximation to the surface deflections. Following the initial estimates, the moduli, viscoelastic constants, and unknown layer thicknesses for each layer were adjusted one at a time on a trial-and-error basis until satisfactory agreement with field data was achieved.

Generally speaking, the responses at the low frequencies are dominated by the lowest layer. This observation led to the introduction of new sublayers by splitting the subgrade or the bedrock, or both, into two sublayers, with modulus increasing with depth. This subdivision improved the correlation at low frequencies.

Section D01S3 was further subjected to an automated backcalculation procedure using the PAVE-SID computer program. The SID study significantly improved agreement of the field data with computed responses. The SID study used frequencies from approximately 10 to 130 Hz in 10-Hz steps.

RESULTS OF COMPARISON STUDY

D01S3 Results

Figure 6 compares SCALPOT-computed values using the backcalculated three-parameter viscoelastic representation with frequency-analyzed FWD data. The symbols represent computed values and the solid line represents the FWD data. The FWD data are the same as in Figure 4. Figures 6a, 6b, 6c, and 6d show the magnitude response at $r = 1$ ft, the phase angle response at $r = 1$ ft, the magnitude response at $r = 4$ ft, and the phase angle response at $r = 4$ ft, respectively. There is good correlation of phase angle at both $r = 1$ ft and $r = 4$ ft. Magnitude correlation is good for $r = 1$ ft; however, some discrepancy is apparent at $r = 4$ ft. Nevertheless, the discrepancy is within 1 mil per 10 kips.

Figure 7 compares, for all displacement sensors at Section D01S3, the SCALPOT-computed values and the frequency-analyzed FWD data shown in Figure 4. It appears here to show the full data set used in the actual backcalculation process. The symbols represent computed values, and the solid lines represent the FWD data. Figures 7a and 7b show the magnitude and phase angle responses, respectively, at $r = 0$, 1, 2, and 3 ft; Figures 7c and 7d show the magnitude and phase angle responses, respectively, at $r = 4$, 5, and 6 ft. There is good agreement for both magnitude and phase angle at all values of r. At a given frequency the magnitudes are larger for smaller values of r, and the phase angles increase with r.

The agreement of the outer sensors in Figure 7c does not appear to be as good as the inner sensors' correlation. This is because the magnitudes are shown on an expanded scale. The absolute correlation for all the magnitudes is within 0.5 to 1 mil per 10 kips, which is the limit of resolution of the geophones. The good overall agreement can be attributed to the use of the PAVE-SID program in the backcalculation.

Table 2 shows pavement layer thicknesses, including the backcalculated thickness of the upper subgrade layer. Table 3 shows viscoelastic parameters E_0, E_1, and n for the AC surface course; backcalculated values for Young's modulus; and damping for the base course and both subgrade layers. Table 4 compares viscoelastic parameters obtained from laboratory tests with those obtained from backcalculation.

D08S4 Results

Figures 8 and 9, respectively, show information for Section D08S4 corresponding to that shown in Figures 6 and 7 for Section D01S3. Again there is good agreement for both magnitude and phase angle for all values of r. Agreement at frequencies below approximately 10 Hz is poor, apparently because of the hyperbolic behavior of the complex modulus in Equation 5b. To avoid this, a four-parameter model for the AC surface course would be necessary.

From coring data, this section was known to have a near-surface bedrock layer at a depth of 9.75 ft (see Table 1). For this reason, the section was initially treated as a four-layered section, with a three-parameter viscoelastic AC layer, a base course, a subgrade layer, and the infinitely deep bedrock layer. In addition to the moduli of the top three layers, the depth to bedrock and the bedrock's modulus were backcal-

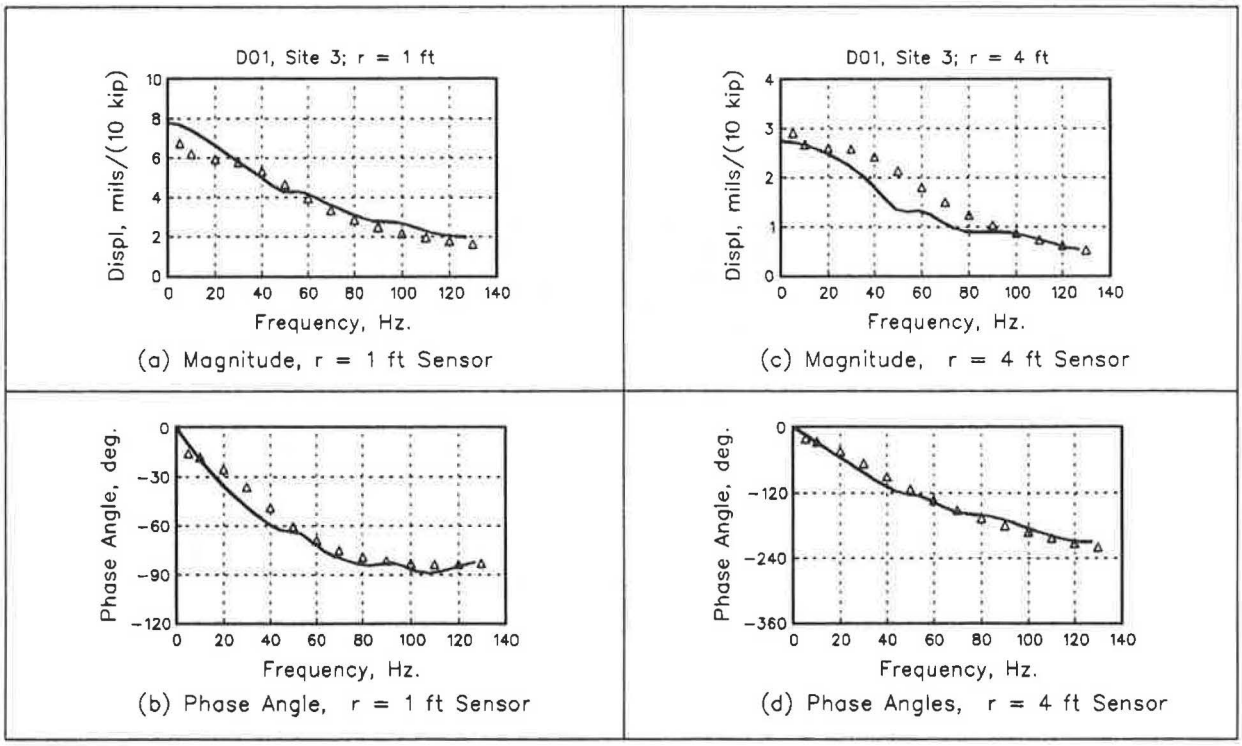

FIGURE 6 D01S3 frequency response functions for $r = 1$ ft and $r = 4$ ft: comparison between computed values (*symbols*) using backcalculated three-parameter viscoelastic representation and frequency-analyzed FWD data (*lines*).

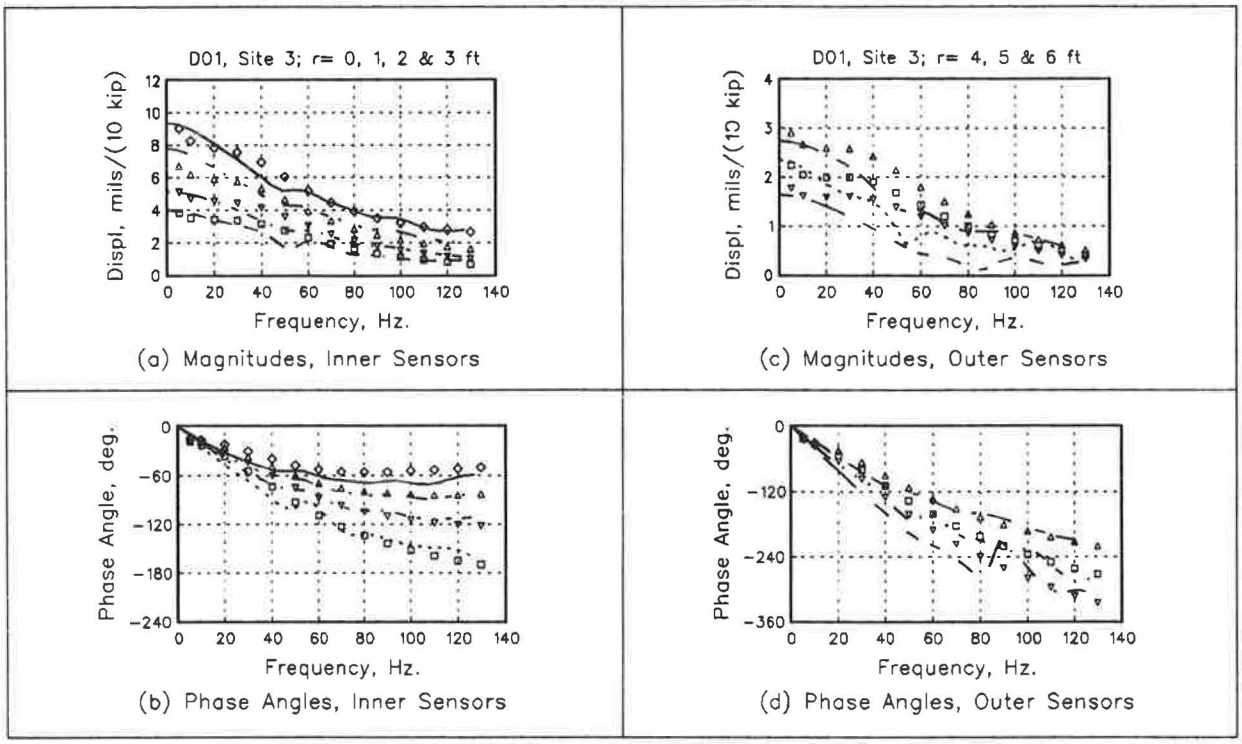

FIGURE 7 D01S3 frequency response functions for all displacement sensors: comparison between computed values (*symbols*) using backcalculated three-parameter viscoelastic representation and frequency-analyzed FWD data (*lines*).

TABLE 2 PAVEMENT LAYER THICKNESS (INCHES)

Site	D01S3		D08S4	
Layer	Thickness	Depth	Thickness	Depth
AC Surface	12	12	10	10
Base	22	34	11	21
Subgrade	20*	54	72*	93
SG-2/BR-1	∞	-	48*	141
Bedrock-2	-	-	∞	-

* Back-Calculated Value

Note: SG indicates subgrade; BR indicates bedrock.

TABLE 3 BACKCALCULATED PAVEMENT LAYER MODULI AND DAMPING

Site	D01S3		D08S4	
Layer	Modulus (KSI)	Damping	Modulus (KSI)	Damping
AC Surf.(3-Par)		0.296*		0.30*
E0	834.0		1250.0	
E1	1516.4		1250.0	
E @ 10 msec	731		999.0	
Base Course	45.11	0.015	104.2	0.015
Subgrade 1	20.17	0.015	31.3	0.075
SG2/BR-1	48.61	0.075	83.33	0.015
Bedrock-2	-	-	111.1	0.015

* Slope of Log-Log Creep Curve

Note: SG indicates subgrade; BR indicates bedrock.

TABLE 4 AC SURFACE COURSE VISCOELASTIC PARAMETERS— LABORATORY DATA AND BACKCALCULATED VALUES

Site	E0 (KSI)	E1 (KSI)	n(slope)
D01S3			
a) Lab, 104°F	2000.0	1666.67	0.5407
b) Back-Calculated	834.0	1516.4	0.296
D08S4			
a) Lab, 104°F	1250.0	312.5	0.6029
b) Back-Calculated	1250.0	1250.0	0.30

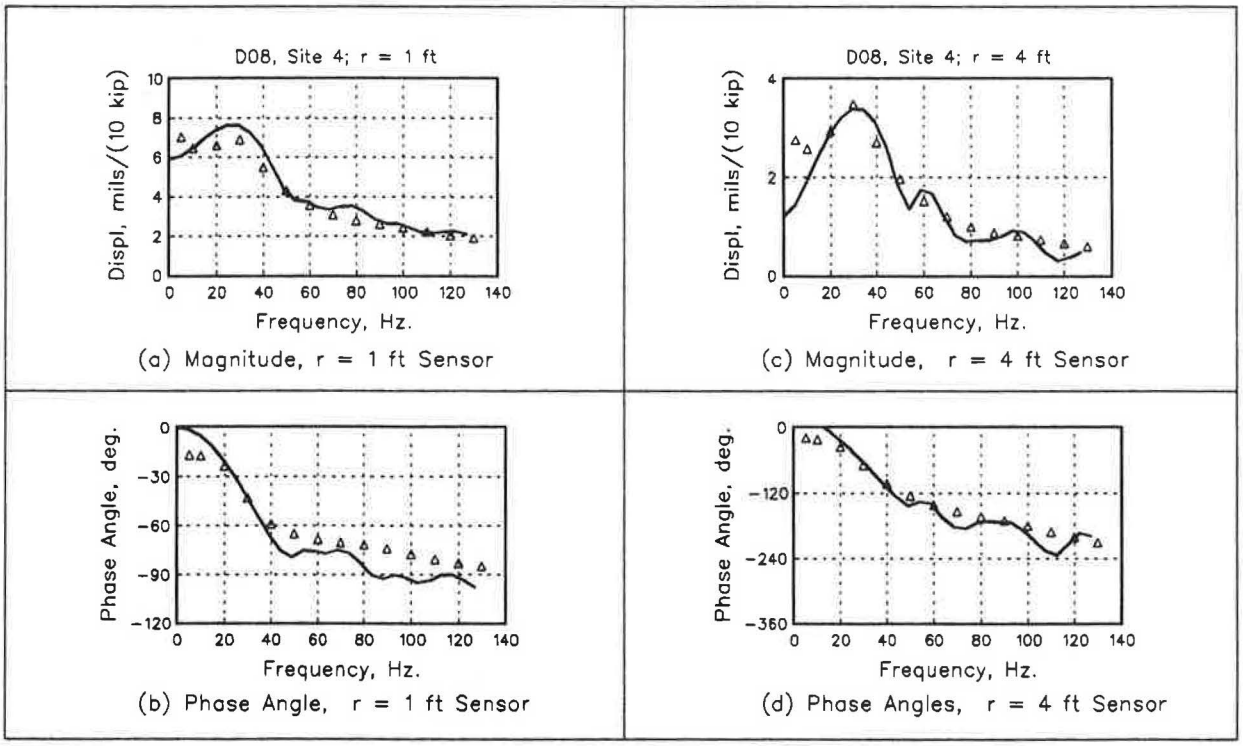

FIGURE 8 D08S4 frequency response functions for $r = 1$ ft and $r = 4$ ft: comparison between computed values (*symbols*) using backcalculated three-parameter viscoelastic representation and frequency-analyzed FWD data (*lines*).

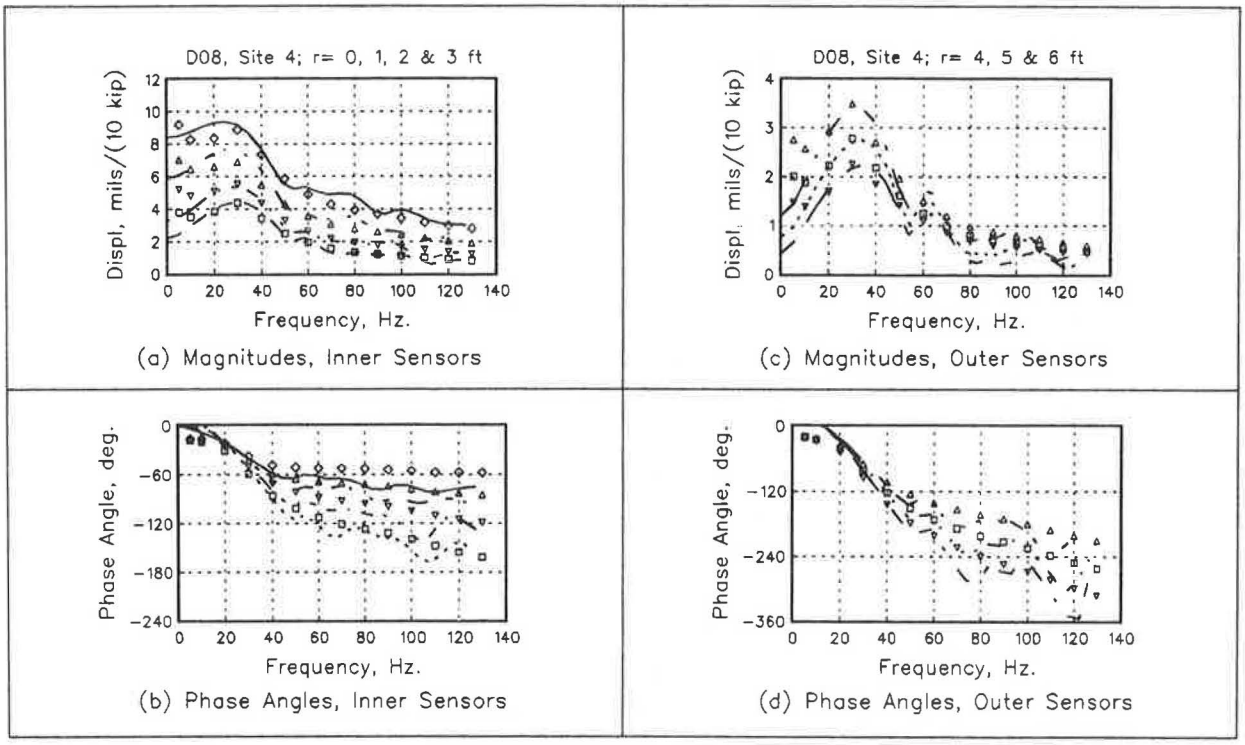

FIGURE 9 D08S4 frequency response functions for all displacement sensors: comparison between computed values (*symbols*) using backcalculated three-parameter viscoelastic representation and frequency-analyzed FWD data (*lines*).

culated. To improve low-frequency agreement, the bedrock half-space was then divided into two layers, as indicated in Table 2. The improved agreement (except at the very low frequencies) is evident in Figures 8 and 9. The good agreement indicates that dynamic analysis can be used to backcalculate pavement layer physical properties, even in the presence of near-surface bedrock. It is clear from the values of the bedrock moduli in Table 3 that any attempt to backcalculate layer properties for this section without taking into account the shallow bedrock would lead to erroneous results.

Comparison Between Laboratory Data and Backcalculated Values

Table 4 compares backcalculated AC viscoelastic parameters and laboratory creep data. The log-log slope (n) for the laboratory data was about twice the backcalculated value for both sections. The backcalculated elastic modulus E_0 was about half the laboratory data value for D01S3, whereas the backcalculated and laboratory data were the same for D08S4. The backcalculated viscoelastic modulus E_1 was about equal to the laboratory data value for D01S3, whereas the backcalculated value was about four times the laboratory data value for D08S4.

Two Versus Three Parameters

The three-parameter viscoelastic model was used instead of the two-parameter model because agreement between laboratory data and backcalculated values was poor for the two-parameter model. The backcalculated slope (n) was typically one-half to one-fifth of the laboratory data value. The backcalculated intercept (A in Equation 1) was typically 1/10th to 1/20th of the laboratory data value. Such large disagreement indicates that the two-parameter model is not physically realistic.

Effective Modulus for AC Surface Layer

The time domain three-parameter complex modulus in Equation 2 may, for comparative purposes, be evaluated at some representative time. The time can be taken at the peak of the FWD drop weight time pulse, which occurs at approximately 10 msec, or 0.01 sec after the start of the pulse (see Figures 1 and 2). Table 3 shows a modulus denoted as "E @ 10 msec" for the AC layer. This representative modulus at the pulse peak can be used to compare with resilient moduli obtained from cyclic loading and resonant column tests.

CONCLUSIONS

The TTI-developed SCALPOT program using a viscoelastic model for the AC surface course has been shown to describe or predict accurately the dynamic responses of the two pavement sections under study, D01S3 and D08S4. For both sections, the program backcalculated pavement layer properties, including moduli, lower layer thicknesses, and, for the AC surface course, the three viscoelastic parameters. On Section D01S3 the subgrade was split into two sublayers for which stiffness increased with depth. This was done to achieve better correlation with the low-frequency FWD data.

The dynamic analysis procedure was used successfully on a pavement section known to have near-surface bedrock, Section D08S4. The FWD responses were shown to be strongly affected by the presence of the near-surface bedrock layer. Nevertheless, the backcalculation produced realistic values for the moduli and the viscoelastic parameters for each layer (including the bedrock layers). The bedrock layer was divided into two sublayers to improve agreement between FWD field data and computed responses at the lower frequencies.

The results described indicate that this dynamic analysis method shows promise for use in the testing and evaluation of AC pavements. The comparison study indicates that pavement dynamic responses can be accurately modeled by adjustment of the physical properties of each layer in the SCALPOT program's input data set.

RECOMMENDATIONS

An extensive validation study is needed to establish the range of pavement types that can be treated by dynamic analysis and the amount and form of engineering information that can be extracted for each type. In such a study laboratory data from samples should be compared with backcalculated pavement layer properties obtained from FWD data, as in Table 4.

Backcalculation studies of 25 Texas pavement sections in the TTI dynamic analysis project are now in progress. The TTI PAVE-SID program will be used to perform automated backcalculations for these sections.

Creep compliance and creep recovery data for AC samples are needed for time scales down to the tens of milliseconds range. These data are required for the three-parameter complex compliance model defined in Equation 5b. The elastic component must be separated from the viscoelastic component. In addition, recoverable deformation must be separated from permanent deformation. The shorter time scales are needed because they are the time scales of the pavement design axle loads at speed. It is not known whether the power-law exponent (n) at the smaller time scales is the same as the exponent at the long time scales customarily used in laboratory creep and creep recovery tests.

This dynamic analysis procedure must be evaluated on its ability to predict layer moduli and viscoelastic parameters, layer thicknesses, and cracking and rutting as they relate to viscoelastic linear and nonlinear properties.

ACKNOWLEDGMENTS

The first author wishes to acknowledge the enthusiastic support, on both technical and financial matters, of his coauthor, the project's technical coordinator, R. C. Briggs of the Texas State Department of Highways and Public Transportation. The first author also wishes to acknowledge his other coauthor, R. L. Lytton, head of TTI's Materials, Pavements and Construction Division, for his guidance on technical matters, encouragement, and support.

George J. Bakas performed the creep tests and provided the creep compliance data. Ajay R. Karkala performed the FWD data reduction and computed the pavement section frequency response functions using the FWD-FFT computer program he developed. Vikram Torpunuri computed the pavement layer properties for Section D01S3 using the PAVE-SID computer program he developed.

REFERENCES

1. R. L. Lytton, F. P. Germann, Y. J. Chou, and S. M. Stoffels. *NCHRP Report 327: Determining Asphaltic Concrete Pavement Structural Properties by Nondestructive Testing*. TRB, National Research Council, Washington, D.C., 1990.
2. J. Uzan, R. L. Lytton, and F. P. Germann. General Procedure for Backcalculating Layer Moduli. *First Symposium on Nondestructive Testing of Pavements and Backcalculation of Moduli*, ASTM, Baltimore, Md., 1988.
3. H. Lamb. On the Propagation of Tremors over the Surface of an Elastic Solid. *Philosophical Transactions of the Royal Society*, Vol. 203, 1904, pp. 1–42.
4. W. M. Ewing, W. S. Jardetzky, and F. Press. *Elastic Waves in Layered Media*. McGraw-Hill Book Company, Inc., New York, 1957.
5. A. H. Magnuson. The Acoustic Response in a Liquid Layer Overlying a Multilayered Viscoelastic Half-Space. *Journal of Sound and Vibration*, Vol. 43, No. 4, 1975, pp. 659–669.
6. A. H. Magnuson. *Sound Propagation in a Liquid Overlying a Viscoelastic Halfspace*. Ph.D. thesis. University of New Hampshire, Durham, 1972.
7. A. H. Magnuson. *Computer Analysis of Falling-Weight Deflectometer Data, Part I: Vertical Displacement Computations on the Surface of a Uniform (One-Layer) Half-Space due to an Oscillating Surface Pressure Distribution*. Research Report 1215-1F. Texas Transportation Institute, Texas A&M University, College Station, Nov. 1988.
8. Y. Zhongjin. A Method of Finite Integrals of Oscillating Functions. *Communications in Applied Numerical Methods*, Vol. 3, 1987, pp.1–4.
9. A. H. Magnuson. *Dynamic Analysis of Falling-Weight Deflectometer Data*. Research Report 1175-1. Texas Transportation Institute, Texas A&M University, College Station, Nov. 1988.
10. V. S. Torpunuri. *A Methodology To Identify Material Properties in Layered Viscoelastic Halfspaces*. M.S. thesis. Texas A&M University, College Station, 1990.
11. W. Menke. Geophysical Data Analysis: Discrete Inverse Theory. *International Geophysics Series*, Vol. 45, 1989.
12. H. G. Natke and J. T. P. Yao. Structural Safety Evaluation Based on System Identification Approaches. *Proceedings of the Structural Safety Evaluation Based on System Identification Approaches*, Lambrecht, Germany, 1988.
13. H. S. Papazian. *The Response of Linear Viscoelastic Materials in the Frequency Domain*. Report 172-2. Transportation Engineering Center, Engineering Experiment Station, Ohio State University, Columbus, 1961.
14. Y. C. Fung. *Foundations of Solid Mechanics*. Prentice-Hall, Inc., Englewood Cliffs, N.J., 1965.
15. J. S. Lai and D. Anderson. Irrecoverable and Recoverable Nonlinear Viscoelastic Properties of Asphalt Concrete. In *Highway Research Record 468*, HRB, National Research Council, Washington, D.C., 1973, pp. 73–88.
16. R. A. Schapery. Nonlinear Fracture Analysis of Viscoelastic Composite Materials Based on a Generalized J Integral Theory. *Proc., Japan-U.S. Conference on Composite Materials*, Tokyo, Jan. 1981.
17. W. J. Kenis. *Predictive Design Procedures, VESYS Users' Manual—An Interim Design Method for Flexible Pavement Using the VESYS Structural Subsystem*. Report FHWA-RE-77-154. FHWA, U.S. Department of Transportation, 1978.